Changes of the aerodynamic characteristics of a flux site after an extensive windthrow

Bruna R. F. Oliveira[1], Jan J. Keizer[1], Thomas Foken[2]

5   [1] Earth surface processes team, Center for Environmental and Marine Studies (CESAM), Department of Environment and Planning, University of Aveiro, Aveiro, Portugal

[2] Bayreuth Center of Ecology and Environmental Research (BayCEER), University of Bayreuth, Bayreuth, Germany

Correspondence to: Thomas Foken (thomas.foken@uni-bayreuth.de)

10   **Abstract.** A maritime pine plantation in Central Portugal that has been continuously monitored using the eddy-covariance technique for carbon fluxes since a wildfire in 2017, was significantly affected by two storms during December 2019 that resulted in a large-sale windthrow. This study analyses the impacts of this windthrow on the aerodynamic characteristics of zero-plane displacement and roughness length, and, ultimately, their implications for the turbulent fluxes. The turbulent fluxes were only affected to a minor degree by the windthrow, but the footprint area of the flux tower changed markedly, so

15   that the target area of the measurements had to be re-determined**.**

Keywords: windthrow, eddy covariance, aerodynamic characteristics, carbon dioxide fluxes

20   **1 Introduction**

Heterogeneous surfaces have an influence on turbulent energy and mass fluxes (Stoy et al., 2013). For example, increased fluxes have been found at forest edges (Klaassen et al., 2002). Large-eddy simulations have suggested that fluxes are at their maximum at a distance of about 10 times the canopy height from the forest edge (Kanani-Sühring and Raasch, 2015;Dupont and Brunet, 2009). An increase in flux could also be associated with an increase in stand heterogeneity (Foken et al., 2021).

25   An intrinsic limitation of the cited studies is that they cannot find a suitable measure of heterogeneity that is correlated with turbulent fluxes.

The post-wildfire flux site in Vila de Rei, central Portugal (Oliveira et al., 2021) offered an opportunity to study the impacts of an abrupt change in aerodynamic characteristics without a concomitant change in stand heterogeneity, virtually like a laboratory experiment. Namely, the storms *Elsa* and *Fabien* caused an extensive windthrow of the - dead - burnt maritime

30   pine trees between 19 and 21 of December 2019, 28 months after the wildfire, while the tumbled trees remained on the ground afterwards (Figure 1). This prompted us to study the changes in the zero-plane displacement and the roughness parameter before and after the windthrow. Furthermore, we decided to analyse if the changes in these two aerodynamic characteristics also affected carbon dioxide fluxes. This question, however, is difficult to answer in this particular case. Roughly two years after the wildfire, the pine ecosystem was still in its initial phase of post-fire vegetation recovery, so that

35   an increase in CO_2 uptake is to be expected between the period before and the period after the windthrow, regardless of the aerodynamic changes. Nevertheless, a change in zero-plane displacement can have a significant impact on the Obukhov-Lettau stability parameter $(z-d)/L$ (z: measurement height, d: zero-plane displacement, L: Obukhov length, Foken and Börngen, 2021), which, in turn, is crucial to the correction and assessment of carbon dioxide fluxes.

2 Materials and methods

2.1 Measurement site and measurements

The measurement area, instrumentation, and data processing were comprehensively described by Oliveira et al. (2021), so only the details essential for this study are given below.

The study area is located 8 km to the southwest of the Vila de Rei municipality, N39° 37' W08° 06', in a Mediterranean climate zone. The wildfire affecting the area burned 1250 ha of woodlands. The measurement site included a plateau of sedimentary sandstone deposits, located at an elevation of 250 m a.s.l. and with slopes of up to 5° over an extension of roughly 10 ha. The crowns of the bulk of the burned maritime pine (*Pinus pinaster* Ait.) were fully consumed by the fire but their trunks of approximately 8 m height remained standing. This canopy height and a zero-plane displacement of 3.8 m were used in all calculations in Oliveira et al. (2021). The localized patches of burned eucalypt trees and stands had a canopy height of approximately 4 m. In the relatively open part of the pine area, a 12m-high slim tower was installed at the end of September 2017 and equipped with an eddy-covariance system at 11.8 m, including a sonic anemometer CSAT3 (Campbell Sci. Inc.) and a LI-7500A gas analyzer (Licor Biosciences), see Figure 1. The fluxes of momentum, sensible heat, latent heat, and carbon dioxide were analyzed with the eddy-covariance method (Aubinet et al., 2012). The data of the eddy-covariance system were calculated with the Campbell Sci. Inc. EasyFlux DL software for a quick inspection in the field, while all further calculations were done with the software package TK3 (Mauder and Foken, 2015).

Figure 1: 12 m slim tower with eddy-covariance system at the burnt Pinus pinaster plantation (left: Photograph: J.J. Keizer, 22 September 2017) and the plantation after the windthrow (right: Photograph: J.J. Keizer, 20 June 2020)

2.2. Aerodynamic characteristics

The starting point for the analysis of the aerodynamic conditions was the logarithmic wind profile. In order to exclude

65   influences due to the stability of the stratification, the analysis was limited to neutral cases ($–0.05 \leq z/L \leq 0.1$). The profile equation contains the measured quantities wind speed u and friction velocity u_* and the two unknowns of zero-plane displacement d and roughness length z_0 (Arya, 2001;Foken, 2017;Stull, 1988)

$$\frac{u(z-d)}{u_*} = \frac{1}{\kappa} \ln \frac{z-d}{z_0} \qquad (1)$$

with the von Kármán constant $\kappa = 0.4$. If wind speeds are measured at different heights, both unknowns can be determined

70   iteratively. In the present case, however, measurements were only available at 11.8 m height, so one of the two parameters must be estimated. It is common in such cases to estimate the zero-plane displacement, in particular as equal to two-thirds of the stand height ($d = 0.666\, z_c$), as is implemented in calculation programs for eddy-covariance measurements. In reality, however, this multiplication factor varies in the range from 0.5 to 0.8, depending on stand structure and, hence, on plant development over the course of a year (Maurer et al., 2015) as well as wind speed (Marunitsch, 1971). Often the value

75   attributed to this factor depends strongly on the experience of the observer. Oliveira et al. (2021) used as canopy height z_c =7.6 m, as zero-plane displacement $d = 3.8$ m $= 0.5\, z_c$, and as roughness length $z_0 = 0.4$ m for the period before the windthrow. For the investigations after the windthrow a canopy height $z_c = 2.7$ m and a zero-plane displacement $d = 1.8$ m $= 0.666\, z_c$ were assumed.

The roughness length and the dimensionless wind profile $u(z-d)/u_*$ are typically used as measures of the roughness of

80   surface and the friction on the surface. In addition, it is useful to determine the so-called integral turbulence characteristic from the standard deviation of the vertical wind velocity and friction velocity σ_w/u_*, which has a value of about 1.25 in the neutral case (Foken, 2017;Garratt, 1992) and of 1.1 for measurements close above the canopy (Finnigan et al., 2009). It can, however, attain higher values under the influence of high roughness (Foken and Leclerc, 2004).

Roughness length can be determined by two methods that are nearly independent. The first method is through Eq. (1) for a

85   given $z - d$:

$$z_0 = \frac{z-d}{e^{\kappa\, u(z-d)/u_*}} \qquad (2)$$

The second method is based on the following relation (Panofsky, 1984), with $\sigma_w/u_* = 1.25$:

$$\frac{\sigma_w}{u(z-d)} = \frac{1.25\, \kappa}{\ln\left(\frac{z-d}{z_0}\right)} \qquad (3)$$

From Eq. (3), roughness length then follows as:

90    $$z_0 = \frac{z-d}{e^{\frac{1.25\, \kappa}{[\sigma_w/u(z-d)]}}} \qquad (4)$$

2.3 Influence of the changes in aerodynamic characteristics on carbon dioxide fluxes

All relevant software packages for the calculation of the carbon dioxide fluxes use, besides measurement height, canopy

95   height and zero-plane displacement as input parameters. These parameters are mainly needed to determine the Obukhov-Lettau stability parameter $(z - d)/L$, with the Obukhov length:

$$L = -\frac{u_*^3}{\kappa \frac{g}{T} \frac{Q_H}{\rho\, c_p}} \qquad\qquad (5)$$

with the gravity accelaration g, the temperature T, the sensible heat flux Q_H, the air density ρ, and the specific heat for constant pressure c_p.

100   The Obukhov-Lettau stability parameter, in turn, is crucial for: (i) spectral correction in the high-frequency spectrum (Garratt et al., 2020;Moore, 1986); (ii) stability-dependent turbulence characteristics in quality control (Foken and Wichura, 1996); and (iii) determination of the footprint (Leclerc and Foken, 2014). Therefore, this study also addresses the implications of the windthow-induced changes in aerodynamics for these three aspects.

The model spectra for frequency correction (e.g. Kaimal et al., 1972) are stability dependent (i), while the integral

105   characteristics used for data quality analysis (if not limited to the neutral case as in Eq. (3)), are also stability dependent (ii), e.g. according to Panofsky et al. (1977):

$$\sigma_w/u_* = 1.3 \left(1 - 2\frac{z-d}{L}\right)^{1/3} \qquad\qquad (6)$$

To determine the source area of CO_2-flux measurements, footprint models (iii) are used, and the input parameters are mainly wind speed, roughness length and stability. In the present case, the widely used model according to Kormann and Meixner

110   (2001) was applied.

Further explanations of the corresponding equations and models shall be omitted, since they are described comprehensively in the literature (Foken et al., 2012;Mauder et al., 2021). Furthermore, supplementary information was provided in the prior publication (Oliveira et al., 2021).

115   **3. Results**

3.1. Aerodynamic characteristics

A climatology of the wind field would require a minimum of 10 years of data, even if a period of 30 years is the standard. In other words, changes in the wind field before and after the windthrow could simply reflect inter-annual variation. Nevertheless, it was striking that the median wind speed was higher after than before the windthrow in eight of the twelve

120   wind sectors (Figure 2), suggesting that the windthrow provoked a generalized decrease in zero-plane displacement.
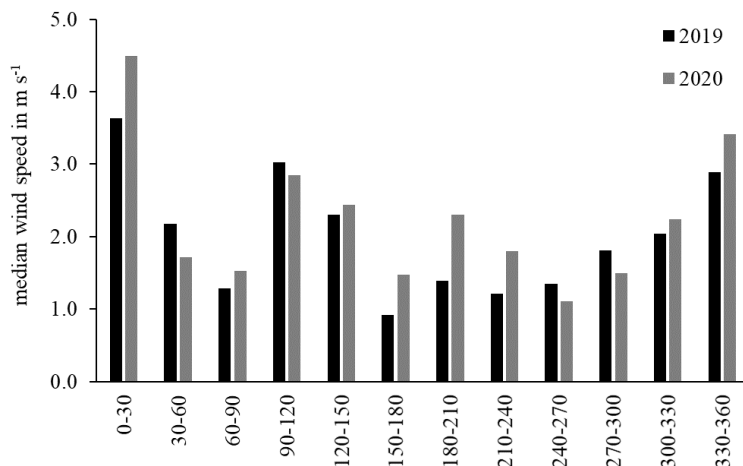
Figure 2: Median wind speed from the 12 wind direction sectors for the periods of May to August 2019 and 2020

According to Table 1, the ratio $u(z-d)/u_*$ before and after the windthrow changed roughly from 5–6 to 8–9, corresponding to about 60% increase. In the NE sector, the change was smaller but the ratio was already comparatively high before the windthrow. Assuming a value for $z-d$ of 8 m before and 10 m after the windthrow, the effective measuring heights were 8 m and 10 m, respectively.

The roughness length showed a decrease after the windthrow (Table 2). Especially after the windthrow, the roughness lengths agreed relatively well between the two methods. Generally, the roughness length was greatest in the SE sector.

The ratio σ_w/u_* showed the expected values (Table 3). The values were slightly lower before than after the windthrow, in line with the smaller distance between measurement height and the top of the canopy. The NE and the W-NW sectors revealed comparatively large roughnesses both before and after the windthrow. The wind sectors highlighted in Tables 1-3 are illustrated in Figure 3.

Table 1: The median of the ratio $u(z-d)/u_*$ before ($z-d$ = 8 m) and after ($z-d$ = 10 m) the windthrow for a nearly nine-month period (22 Dec. 2018 to 30 Sept. 2019 and 22 Dec. 2019 to 30 Sept. 2020)

	0–30	30–60	60–90	90–120	120–150	150–180	180–210	210–240	240–270	270–300	300–330	330–360
Wind direction												
Before windthrow	5.25	6.69	7.38	5.97	5.15	5.26	6.48	5.77	5.79	6.98	6.26	5.51
After windthrow	8.47	8.74	9.52	7.64	6.60	8.27	9.19	9.16	8.71	10.13	8.51	8.03

Table 2: The median roughness lengths z_0 in m before ($z - d = 8$ m) and after ($z - d = 10$ m) the windthrow for the nearly nine-month periods, computed following Eqs. (2) and (4)

Wind direction	0–30	30–60	60–90	90–120	120–150	150–180	180–210	210–240	240–270	270–300	300–330	330–360
Before windthrow												
Eq. 2	0.98	0.55	0.42	0.73	1.02	0.98	0.60	0.80	0.79	0.49	0.65	0.88
Eq. 4	0.89	0.73	0.38	0.59	0.86	0.81	0.48	0.55	0.65	0.50	0.61	0.79
After windthrow												
Eq. 2	0.34	0.30	0.22	0.47	0.71	0.37	0.25	0.26	0.31	0.17	0.33	0.40
Eq. 4	0.27	0.40	0.26	0.36	0.57	0.41	0.23	0.22	0.28	0.22	0.34	0.34

140

Table 3: The median ratio σ_w/u_* before ($z - d = 8$ m) and after ($z - d = 10$ m) the windthrow for the nearly nine-month periods

Wind direction	0–30	30–60	60–90	90–120	120–150	150–180	180–210	210–240	240–270	270–300	300–330	330–360
Before windthrow	1.20	1.39	1.21	1.15	1.15	1.15	1.15	1.07	1.15	1.26	1.22	1.19
After windthrow	1.17	1.36	1.31	1.15	1.15	1.30	1.22	1.21	1.22	1.33	1.26	1.19
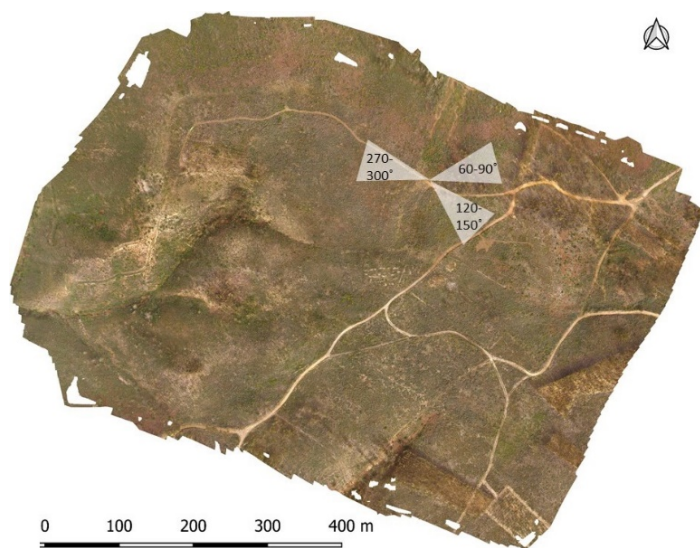
145

Figure 3: Unmanned Aerial System (UAS)-based ortho-photomap with the most disturbed wind sectors. Image from 23 February 2021 by B.R.F. Oliveira.

3.2 Influence on Carbon dioxide fluxes

150

Carbon dioxide fluxes were evaluated for the months of May to August 2019 and 2020 to investigate the impacts of the windthrow-induced changes in the stability parameter. This was done without gap-filling. Of course, the comparison between before- and after-windthrow fluxes is not straightforward, because of the differences in weather conditions as well as in post-fire ecoystem recovery between the two periods. Therefore, the spectral correction and data quality analysis were only done for the 2020 data set, assuming two different zero-plane displacements.

155

Examination of the ratio σ_w / u_* showed minor and not relevant differences for $z - d = 8$ m before the wind break and $z - d = 10$ m m after the windthrow. The median differed by only 0.4 % and, hence, did not affect the quality flagging. Also the difference with and without spectral correction was reduced, even if slightly over 1 %.

A similar result was obtained for the CO_2 and net ecosystem exchange (NEE) fluxes. As shown in Figure 4, the differences in NEE fluxes with and without stratification-dependent spectral correction was about 1% for the two different effective measurement heights 8 m and 10 m. The median values of the spectrally corrected fluxes differed less than 0.5 % between both measurement heights. Furthermore, the scatter around these median values was reduced.

160
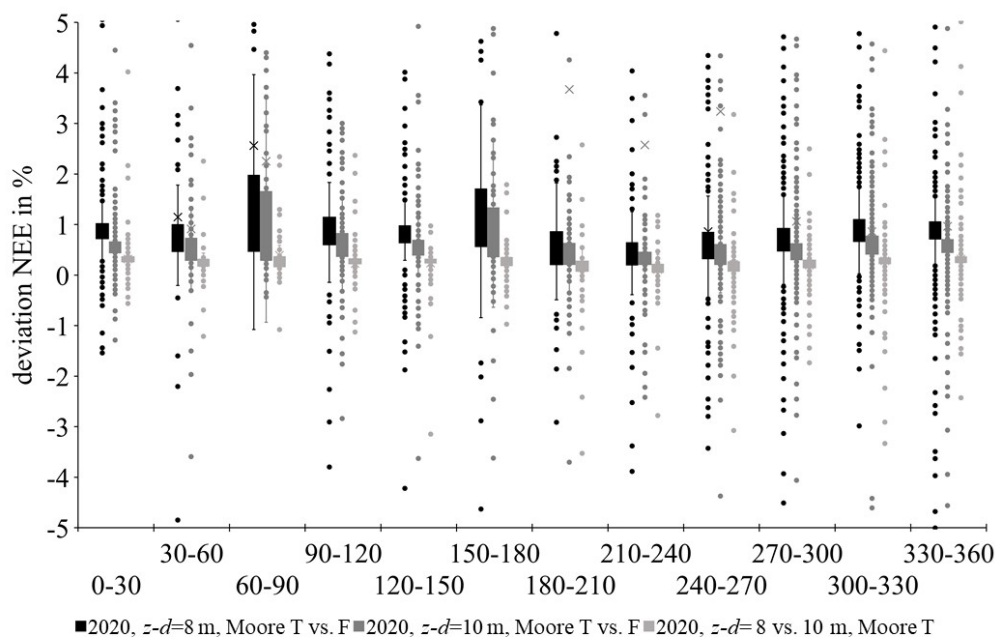
Figure 4: Comparison of the net ecosystem excahnge (NEE) with and without spectral correction for $z - d = 8$ m (Moore T=used vs F=not used) and $z - d = 10$ m (Moore T vs F) and with spectral correction for both effective measuring heights (Moore T, $z - d = 8$ m vs 10 m) for the dataset from May to September 2020

165

More pronounced implications were expected with respect to the size of the source area. Therefore, the target area of burned pine woodland with down wood of charred trunks was calculated with the footprint model (Kormann and Meixner, 2001) ,

170 analogous to Oliveira et al. (2021). For ther 2020 period, this was done for both values of $z - d = 8$ and $z - d = 10$ and the assigned roughness lengths of $z_0 = 0.7$ m and $z_0 = 0.3$ m before and after the windthrow, respectively (Figure 5) . For comparison, Figure 5 also shows the results for the 2019 period. The differences between the results obtained using $z - d = 8$ m and $z_0=0.7$ m for both periods were mainly due to the differences in wind regimes during the 2019- and 2020-periods, as shown in Figure 2. The differences between the results obtained for the 2020-period using the different aerodynamic

175 parameter values of before and after the windthrowwere relevant. The footprint was substantially larger for the post- than pre-windthrow parameter values, while the number of cases with the target area in the footprint was clearly smaller.

The enlargement of the footprint can be prevented by reducing the measuring height. This is usually not possible with long-term measurement programmes with a permanently installed mast, because then you get flow distortion problems due to the mast. Hydraulic lifted masts are hardly ever used in such programmes (Kolle et al., 2021). To simulate this case, Figure 5

180 shows the footprint for a measurement height of 9.8 m with a reduction of the wind speed by 10 % (z-d = 8 m, z_0 =0.3 m). The change in measurement height leads to an almost identical distribution of the footprint as before the windthrow in 2019.
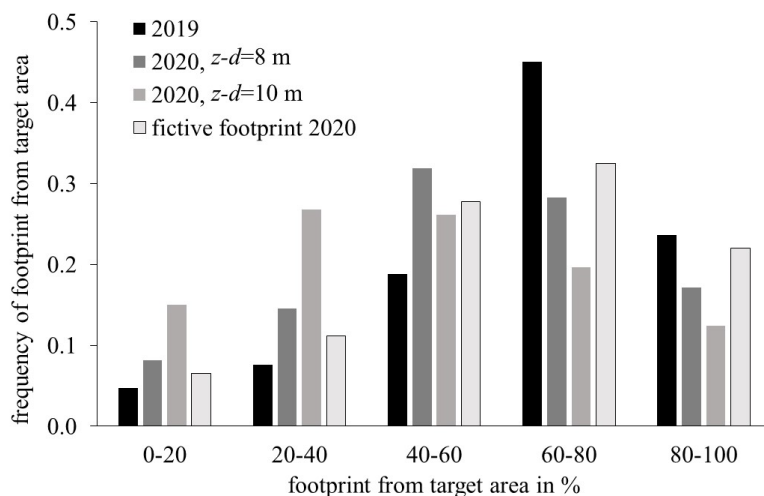
Figure 5: Percentage of the target area (*burnt maritime pine woodland*) classes in the footprint area of the eddy-
185 **covariance measurements from May to August 2019 and 2020, using $z - d = 8$ m for both periods and $z - d = 10$ m for the 2020-period. Furthermore, the fictive footprint for a measurement height of 9.8 m with a reduction of the wind speed by 10 % (z-d = 8 m, z_0 =0.3 m) is shown.**

4. Discussion

190 ### 4.1. Aerodynamic characteristics

Before the windthrow, the wind profile was lifted up by the displacement height. After the windthrow, the tumbled pine trees determined the roughness. However, the roughness was slightly lower after windthrow, while the typical directional dependence was largely preserved. The two determination methods produced consistent results. Worth stressing is that the two methods (Eq. 2 and 4) are not completely independent, because they can be transformed into each other.

195   The 120°-150° sector had a comparatively high roughness both before and after the windthrow. This was probably due to the greater slope angle or the influence of the tower. By contrast, the 30°–60° and 270°–300° sectors were affected by additional mechanical turbulence, as was also found by Oliveira et al. (2021) for the first post-fire year. This is illustrated in Figure 6, using Eq. (1), and shows the dimensionless wind profile as a function of $z - d$ for different roughness lengths. Also the median values for the 30° sectors were included in the plot. Because of the physical correlation between all quantities,

200   the plot cannot be used to determine the zero-plane displacement (as referred earlier) but it does indicate the sectors where the assumed parameter values seem appropriate.
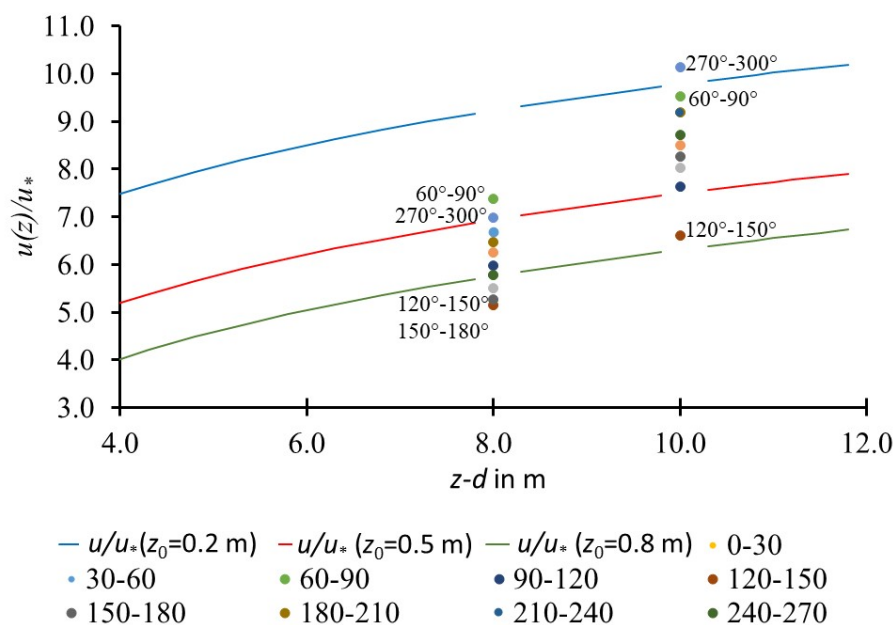
Figure 6: Normalized wind profile in dependence on the displacement height given as $z - d$ ($z = 11.8$ m) and the roughness length z_0. Median values for wind sectors are plotted for $z - d = 8$ m (before the wind break) and $z - d =$

205   **10 m (after the wind break).**

The ratio σ_w / u_* was largely constant at neutral stratification and only revealed a small stability dependence. This parameter can be used to detect obstacles at larger distances (Foken and Leclerc, 2004) or near the anemometer, for example. Even single standing trees can generate noticeable mechanical turbulence (Jegede and Foken, 1999). In the 60°–90° sector, the

210   mechanical turbulence was probably due to eucalypt trees, whose crowns were quickly re-established after the wildfire by

resprouting. The increased values in the 270°–330° sector can only be explained by slope parallel flow, see Oliveira et al. (2021), Figure 1.

Evaluation of both dimensionless parameters, together with an assessment of terrain and post-fire vegetation recovery, suggested that the assumptions in (Oliveira et al., 2021) of $z - d = 8$ m and $z_0 = 0.4$ m were adequate for most wind sectors for the post-fire and pre-windthrow period. However, a value for $z_0 = 0.7$ m would have more appropriate for the calculation of the footprint. Likewise, the assumptions of $z - d = 10$ m and $z_0 = 0.3$ m were appropriate for most wind sectors for the post-windthrow period. These assumptions, however, were less approriate for three sectors highlighted in Table 3, most notably after the windthrow, where no increase in the wind speed (Figure 2) could be detected. The greater variability in roughness after the windthrow can be explained by the higher wind speeds which, in turn, were due to the increase in effective measurement height resulting from the larger distance to the canopy height.

4.2 Influence on Carbon-dioxide fluxes

The investigations carried out clearly showed that due to the different values of the effective measurement height $z - d$ before and after the wind break in the determination of the Obukhov-Lettau stability parameter, no influence on the quality flags and the measurement of the net ecosytem exchange could be detected that would have even come close to the typical error range.

By contrast, however, the footprint area increased markedly due to the change in roughness and possibly also wind speed. The difference would probably not have been as large if a slightly better value of $z_0 = 0.5$ m had been assumed before the windthrow. The increase in footprint area also implied a decrease of the target areas in the footprint. In case target areas differ markedly from non-target areas in terms of carbon dioxide fluxes, the change in aerodynamic conditions would substantially affect flux measurements. At the present study site, this is probably not the case, as the non-target areas mainly differ from the target areas by their greater slope angles and not the burned forest.

5. Conclusions

The windthrow at the end of 2019 had a significant impact on the aerodynamics of the study area. The present analysis addressed dimensionless turbulence characteristics and focused on the parameters of roughness length and zero-plane displacement. Since both parameters are not independent, either the zero-plane displacement or the roughness length must be specified a priori. For the first post-fire year, Oliveira et al. (2021) selected a $d = 3.8$ m $= 0.5\ z_c$ ($z - d = 8$ m), justified by the open character of the burnt pine stand due to the complete consumption of most pine crowns by the wildfire. The authors' assumption of $z_0 = 0.4$ m, however, should be revised to $z_0 = 0.7$ m.

The initial assumption of this study of $z - d = 10$ m and a roughness length of $z_0 = 0.3$ m for the post-windthrow period continues to seem reasonable as well.. This implied that the windthrow drastically changed aerodynamic site conditions. The increase in σ_w/u_* provided a clear indication that the distance between measurement height and canopy height had increased significantly after the windthrow.

The present study confirmed the disturbances in specific wind sectors signalled by Oliveira et al. (2021). The disturbances in the NE and NW sectors could be assigned to terrain characteristics. According to Figure 6, a change in zero-plane displacement in this sector would not result in an improvement. If coordinate rotation is performed by means of double rotation (Kaimal and Finnigan, 1994), the problem is hardly relevant for the measurements; however, when it is done by means of planar fit rotation (Wilczak et al., 2001), the disturbed sector would have to be rotated separately.

250

The change in aerodynamic conditions due to the windthrow did not have marked impacts on the calculation of the carbon dioxide fluxes, but it did substantially increase the footprint area. In the present case, this increase in footprint area implied the inclusion of sloping terrain but with essentially the same pre- and post-fire vegetation cover as the realtively flat target area, so that the implications are expected to be minor. The present windthrow occurred at a relative early stage of post-fire ecosystem recovery, so that a direct comparison of pre- and post-windthrow carbon dioxide fluxes was considered unwarranted.

255

Based on the investigation carried out, we generally recommend determining the effective measurement height and the roughness length as precisely as possible when aerodynamic conditions change in order to be able to determine changes in the footprint area. Since areas outside the target area may have an influence on the fluxes, the quality assessment of the measurement area must be carried out again, taking the footprint into account (Foken et al., 2012;Mauder et al., 2021). Alternatively, the measurement height could be adjusted so that the footprint remains almost identical.

260

Code and data availability. The program for the calculation of the eddy-covariance data is available (Mauder and Foken, 2015). The daily CO_2 flux data are available on Oliveira et al. (2020), other data on request from the first author (bruna.oliveira@ua.pt).

265

Authors contribution. BRFO was the responsible for ModelEco's project funding and management, and responsible scientist for this Post-doctoral study including fieldwork, data analysis (CO_2-part), and preparing the structure of the paper and of several of its sections; JJK was responsible for FIRE-C-BUDs' project funding and management, and data analysis (wind-part), and revised the paper. TF was the scientific adviser of the project, mainly for the flux part and special aerodynamic analysis, and supported the writing of the paper. The final version of the paper was prepared by all authors.

270

Competing interests. The authors declare that they have no conflict of interest.

275

Acknowledgements. This work was supported by the projects ModelEco (PTDC/ASP-SIL/3504/2020), funded by national funds (OE) through FCT/MCTES, and FIRE-C-BUDs (PTDC/AGR-FOR/4143/2014 - POCI-01-0145-FEDER-016780), funded by the FCT/MEC with co-funding by the FEDER, within the PT2020 Partnership Agreement and Compete 2020. Thanks are due to FCT/MCTES for the financial support to CESAM (UIDP/50017/2020+UIDB/50017/2020), through national funds. This publication was funded by the German Research Foundation (DFG) and the University of Bayreuth within the funding program Open Access Publishing.

280

Edited by:

References

285

Arya, S. P.: Introduction to Micrometeorology, Academic Press, San Diego, 415 pp., 2001.

Aubinet, M., Vesala, T., Papale, D. (eds.): Eddy Covariance: A Practical Guide to Measurement and Data Analysis, Springer, Dordrecht, 438 pp, doi: 10.1007/978-94-007-2351-1, 2012

Dupont, S., and Brunet, Y.: Coherent structures in canopy edge flow: a large-eddy simulation study, J. Fluid Mech., 630, 93-128, doi: 10.1017/S0022112009006739, 2009.

290

Finnigan, J. J., Shaw, R. H., and Patton, E. G.: Turbulence structure above a vegetation canopy, J. Fluid Mech., 637, 687-424, doi: 10.1017/S0022112009990589, 2009.

Foken, T., and Wichura, B.: Tools for quality assessment of surface-based flux measurements, Agric. For. Meteorol., 78, 83-105, doi: 10.1016/0168-1923(95)02248-1, 1996.

Foken, T., and Leclerc, M. Y.: Methods and limitations in validation of footprint models, Agric. For. Meteorol., 127, 223-234, doi: 10.1016/j.agrformet.2004.07.015, 2004.

295

Foken, T., Leuning, R., Oncley, S. P., Mauder, M., and Aubinet, M.: Corrections and data quality in: Eddy Covariance: A Practical Guide to Measurement and Data Analysis, edited by: Aubinet, M., Vesala, T., and Papale, D., Springer, Dordrecht, Heidelberg, London, New York, 85-131, doi: 10.1007/978-94-007-2351-1_4, 2012.

Foken, T.: Micrometeorology, 2nd ed., Springer, Berlin, Heidelberg, 362 pp., doi: 10.1007/978-3-642-25440-6, 2017.

300

Foken, T., Babel, W., Munger, J. W., Grönholm, T., Vesala, T., and Knohl, A.: Selected breakpoints of net forest carbon uptake at four eddy-covariance sites, Tellus B: Chemical and Physical Meteorology, 73, 1-12, doi: 10.1080/16000889.2021.1915648, 2021.

Foken, T., and Börngen, M.: Lettau's Contribution to the Obukhov Length Scale: A Scientific Historical Study, Boundary-Layer Meteorol., 179, 369-383, doi: 10.1007/s10546-021-00606-4, 2021.

Garratt, J., Wilczak, J., Holtslag, A., Schmid, H. P., Grachev, A., Beljaars, A., Foken, T., Chen, F., Fairall, C., Hicks, B., Kusaka, H., Martilli, A., Masson, V., Mauder, M., Oncley, S., Rotach, M., and Tjernström, M.: Commentaries on Top-Cited Boundary-Layer Meteorology Articles, Boundary-Layer Meteorol., 177, 169-188, doi: 10.1007/s10546-020-00563-4, 2020.

305

Garratt, J. R.: The Atmospheric Boundary Layer, Cambridge University Press, Cambridge, 316 pp., doi, 1992.

Jegede, O. O., and Foken, T.: A study of the internal boundary layer due to a roughness change in neutral conditions observed during the LINEX field campaigns, Theor. Appl. Climat., 62, 31-41, doi: 10.1007/s007040050072, 1999.

310

Kaimal, J. C., Wyngaard, J. C., Izumi, Y., and Coté, O. R.: Spectral characteristics of surface layer turbulence, Quart. J. Roy. Meteorol. Soc., 98, 563-589, doi: 10.1002/qj.49709841707, 1972.

Kaimal, J. C., and Finnigan, J. J.: Atmospheric Boundary Layer Flows: Their Structure and Measurement, Oxford University Press, New York, NY, 289 pp., doi: 10.1093/oso/9780195062397.001.0001, 1994.

Kanani-Sühring, F., and Raasch, S.: Spatial variability of scalar concentrations and fluxes downstream of a clearing-to-forest transition: A Large-Eddy Simulation study, Boundary-Layer Meteorol., 155, 1-27, doi: 10.1007/s10546-014-9986-3, 2015.

315

Klaassen, W., van Breugel, P. B., Moors, E. J., and Nieveen, J. P.: Increased heat fluxes near a forest edge, Theor. Appl. Climat., 72, 231-243, doi, 2002.

Kolle, O., Kalthoff, N., Kottmeier, C., and Munger, J. W.: Ground based platforms, in: Springer Handbook of Atmospheric Measurements, edited by: Foken, T., Springer Nature, Switzerland, 155-182, doi: 10.1007/978-3-030-52171-4_6, 2021.

320

Kormann, R., and Meixner, F. X.: An analytical footprint model for non-neutral stratification, Boundary-Layer Meteorol., 99, 207-224, doi: 10.1023/A:1018991015119, 2001.

Leclerc, M. Y., and Foken, T.: Footprints in Micrometeorology and Ecology, Springer, Heidelberg, New York, Dordrecht, London, XIX, 239 pp., doi: 10.1007/978-3-642-54545-0, 2014.

325

Marunitsch, S. V.: Charakteristiki turbulentnosti v yslovijach lesa po gradientnym i strukturnym nabljudenijam (Turbulence characteristics of gradients in a forest from structure observations), Trudy Gos. Gidrometeorol. Inst., 198, 154-165, doi, 1971.

Mauder, M., and Foken, T.: Eddy-Covariance software TK3, Zenodo, 10.5281/zenodo.20349 doi: 10.5281/zenodo.20349, 2015.

Mauder, M., Foken, T., Aubinet, M., and Ibrom, A.: Eddy-Covariance Measurements, in: Springer Handbook of Atmospheric Measurements, edited by: Foken, T., Springer Nature, Switzerland, 1473-1504, doi: 10.1007/978-3-030-51171-4_55, 2021.

330 Maurer, K. D., Bohrer, G., Kenny, W. T., and Ivanov, V. Y.: Large-eddy simulations of surface roughness parameter sensitivity to canopy-structure characteristics, Biogeosci., 12, 2533-2548, doi: 10.5194/bg-12-2533-2015, 2015.

Moore, C. J.: Frequency response corrections for eddy correlation systems, Boundary-Layer Meteorol., 37, 17-35, doi: doi:10.1007/BF00122754, 1986.

Oliveira, B. R. F., Keizer, J. J., and Foken, T.: Daily Carbon Dioxide fluxes measured by an eddy-covariance station in a recently burnt
335 Mediterranean pine stand in Central Portugal, PANGAEA, doi: 10.1594/PANGAEA.921281, 2020.

Oliveira, B. R. F., Schaller, C., Keizer, J. J., and Foken, T.: Estimating immediate post-fire carbon fluxes using the eddy-covariance technique, Biogeosci., 18, 285-302, doi: 10.5194/bg-18-285-2021, 2021.

Panofsky, H. A., Tennekes, H., Lenschow, D. H., and Wyngaard, J. C.: The characteristics of turbulent velocity components in the surface layer under convective conditions, Boundary-Layer Meteorol., 11, 355-361, doi: 10.1007/BF02186086, 1977.

340 Panofsky, H. A.: Vertical variation of roughness length at the Boulder Atmospheric Observatory, Boundary-Layer Meteorol., 28, 305-308, doi: 10.1007/BF00121309, 1984.

Stoy, P. C., Mauder, M., Foken, T., Marcolla, B., Boegh, E., Ibrom, A., Arain, M. A., Arneth, A., Aurela, M., Bernhofer, C., Cescatti, A., Dellwik, E., Duce, P., Gianelle, D., van Gorsel, E., Kiely, G., Knohl, A., Margolis, H., McCaughey, H., Merbold, L., Montagnani, L., Papale, D., Reichstein, M., Serrano-Ortiz, P., Sottocornola, M., Saunders, M., Spano, D., Vaccari, F., and Varlagin, A.: A data-
345 driven analysis of energy balance closure across FLUXNET research sites: The role of landscape-scale heterogeneity, Agric. For. Meteorol., 171-172, 137-152, doi: 10.1016/j.agrformet.2012.11.004, 2013.

Stull, R. B.: An Introduction to Boundary Layer Meteorology, Kluwer, Dordrecht, 666 pp., doi: 10.1007/978-94-009-3027-8, 1988.

Wilczak, J. M., Oncley, S. P., and Stage, S. A.: Sonic anemometer tilt correction algorithms, Boundary-Layer Meteorol., 99, 127-150, doi: 10.1023/A:1018966204465, 2001.

350